Virology 483 (2015) 264–274

Contents lists available at ScienceDirect

Virology

journal homepage: www.elsevier.com/locate/yviro

ATM facilitates mouse gammaherpesvirus reactivation from myeloid cells during chronic infection

Joseph M. Kulinski [a], Eric J. Darrah [a], Katarzyna A. Broniowska [b], Wadzanai P. Mboko [a], Bryan C. Mounce [a], Laurent P. Malherbe [c], John A Corbett [b], Stephen B. Gauld [d,1], Vera L. Tarakanova [a,e,*]

[a] Microbiology and Molecular Genetics, United States
[b] Biochemistry, Medical College of Wisconsin, United States
[c] Blood Research Institute, Blood Center of Wisconsin, United States
[d] Division of Allergy and Clinical Immunology, Department of Pediatrics, United States
[e] Cancer Center, Medical College of Wisconsin, 8701 Watertown Plank Road, Milwaukee, WI 53226, United States

ARTICLE INFO

Article history:
Received 2 March 2015
Returned to author for revisions
22 March 2015
Accepted 30 April 2015
Available online 21 May 2015

Keywords:
ATM
Gammaherpesvirus
Myeloid cell
T cell response
Reactivation

ABSTRACT

Gammaherpesviruses are cancer-associated pathogens that establish life-long infection in most adults. Insufficiency of Ataxia-Telangiectasia mutated (ATM) kinase leads to a poor control of chronic gammaherpesvirus infection via an unknown mechanism that likely involves a suboptimal antiviral response. In contrast to the phenotype in the intact host, ATM facilitates gammaherpesvirus reactivation and replication *in vitro*. We hypothesized that ATM mediates both pro- and antiviral activities to regulate chronic gammaherpesvirus infection in an immunocompetent host. To test the proposed proviral activity of ATM *in vivo*, we generated mice with ATM deficiency limited to myeloid cells. Myeloid-specific ATM deficiency attenuated gammaherpesvirus infection during the establishment of viral latency. The results of our study uncover a proviral role of ATM in the context of gammaherpesvirus infection *in vivo* and support a model where ATM combines pro- and antiviral functions to facilitate both gammaherpesvirus-specific T cell immune response and viral reactivation *in vivo*.

Introduction

The human gammaherpesviruses Kaposi's sarcoma-associated herpesvirus (KSHV) and Epstein–Barr virus (EBV) are ubiquitous pathogens that are associated with the development of lympho-proliferative disorders and other malignancies (Cesarman, 2011). Increased viral reactivation from latency is associated with increased risk of developing KSHV- or EBV-driven cancers (Campbell et al., 2000; Meerbach et al., 2008; Feng et al., 2004; Orlandi et al., 2001). Therefore, identification of host factors that suppress or promote viral reactivation *in vivo* is likely to offer an important insight into the mechanism of gammaherpesvirus-driven lymphomagenesis. Unfortunately, identification of such host factors is hindered by the species restriction of human gammaherpesviruses. Mouse gammaherpesvirus 68 (MHV68) is genetically and biologically related to EBV and KSHV (Efstathiou et al., 1990; Virgin et al., 1997; Tarakanova et al., 2005) and offers a powerful small animal model that allows identification of host factors that regulate chronic gammaherpesvirus infection *in vivo*.

ATM is a multifunctional kinase that was originally defined as a critical component of the DNA damage response (Savitsky et al., 1995; Lavin, 2008). Mutations of ATM are a hallmark of Ataxia-Telangiectasia (A-T), a debilitating and progressive disease in which life expectancy is limited to the first two decades. ATM insufficiency is associated with decreased numbers of circulating B and T cells; thus, many (but not all) A-T patients fall under the clinical definition of immune deficiency (Nowak-Wegrzyn et al., 2004). While A-T patients are more susceptible to respiratory bacterial infections (Morio et al., 2009; Nowak-Wegrzyn et al., 2004), these patients can clear most acute viral infections and are successfully and uneventfully immunized with many live attenuated virus vaccines (Nowak-Wegrzyn et al., 2004). Accordingly, ATM deficient mice clear acute Lymphocytic Choriomeningitis virus (LCMV) infection with the same kinetics as wild type animals (D'Souza et al., 2011b). In contrast, A-T patients display increased

* Corresponding author at: Microbiology and Molecular Genetics, Medical College of Wisconsin, 8701 Watertown Plank Road, Milwaukee, WI, 53226, United States. Tel.: +1 414 955 7480; fax: +1 414 955 6535.
E-mail address: vera@mcw.edu (V.L. Tarakanova).
[1] Current address: Abbvie, Dermatology, 1 North Waukegan Road, North Chicago, IL 60064, United States.

http://dx.doi.org/10.1016/j.virol.2015.04.026
0042-6822/

susceptibility to severe infections caused by all three classes of herpesviruses (Folgori et al., 2010; Lankisch et al., 2013; Masucci et al., 1984;Morio et al., 2009; Nowak-Wegrzyn et al., 2004; Saemundsen et al., 1981; Ben-Zvi et al., 1978), suggesting that ATM selectively suppresses chronic herpesvirus infection. Specifically, primary Varicella-Zoster virus infection is more severe in A-T patients, with 5% of patients requiring hospitalization, and herpes zoster incidence is increased in this patient cohort (Folgori et al., 2010; Nowak-Wegrzyn et al., 2004). Similarly, viral loads of human herpesvirus 6 are significantly elevated in A-T patients (Lankisch et al., 2013). Consistent with the focus of this study, A-T patients uniformly display high Epstein–Barr virus (EBV) viral loads; furthermore, uncontrolled EBV-driven lymphoproliferation in children has been suggested as a diagnostic trigger for A-T that frequently presents with otherwise subtle symptoms early in life (Lankisch et al., 2013). Patients with related chromosomal instability syndromes, such as Nijmegen Breakage syndrome, share the inability to properly control chronic gamma- and betaherpesvirus infections (Lankisch et al., 2013; Gregorek et al., 2010). Importantly, the mechanism by which ATM regulates herpesvirus infection has not been explored.

Consistent with the clinical presentation in humans, we showed increased MHV68 reactivation and persistent replication in chronically infected ATM deficient mice along with an altered virus-specific CD8 T cell response (Kulinski et al., 2012). Intriguingly, in contrast to the elevated MHV68 reactivation in ATM deficient mice, ATM facilitates MHV68 replication in primary macrophages *in vitro* (Tarakanova et al., 2007), supports EBV reactivation from several latently infected cancer cell lines (Hagemeier et al., 2012a), and promotes the establishment of KSHV latency in endothelial cells *in vitro* (Singh et al., 2013). To reconcile these opposing ATM phenotypes, we hypothesized that ATM supports viral reactivation within infected cells in addition to promoting the development of gammaherpesvirus-specific adaptive immune response that limits viral reactivation, establishing a delicate balance between anti- and proviral activities *in vivo*.

To test potential proviral functions of ATM *in vivo*, we developed a mouse model of myeloid-specific ATM deficiency. While myeloid cell-restricted ATM deficiency had no effect on the generation of a gammaherpesvirus-specific T cell response, it attenuated MHV68 reactivation and reservoir during the establishment of chronic infection. These data support the model whereby ATM regulates chronic gammaherpesvirus infection by balancing its proviral functions within myeloid cells and antiviral functions within the adaptive virus-specific immune response.

Results

Mouse model of myeloid cell-specific ATM deficiency.

To achieve myeloid cell-specific ATM deficiency, conditional ATM alleles (Zha et al., 2008) were combined with a knock in allele where expression of Cre recombinase was driven by the endogenous lysozyme 2 promoter (Clausen et al., 1999) (designated as M-Cre). To retain expression of the endogenous lysozyme 2 gene, mice were maintained as heterozygotes for the M-Cre allele. M-Cre positive, bone marrow derived macrophages showed a decrease in the relative abundance of the intact *atm delta Cre* locus with a corresponding increase in the recombined *atm* allele (Fig. 1B; schematic of the conditional allele and primers used for analyses are shown in Fig. 1A). Consistent with genetic recombination, ATM protein levels were below the level of detection in M-Cre positive as compared to M-Cre negative macrophages *in vitro* (Fig. 1C). To assess ATM depletion *in vivo*, peritoneal cells were harvested from M-Cre positive and negative mice. ATM protein was detected in sorted peritoneal macrophages ($CD11c^{-}CD11b^{+}F4/80^{+}$) harvested from M-Cre negative but not M-Cre positive mice (Fig. 1D, E), validating the myeloid cell-specific mouse model of ATM deficiency.

Myeloid cell-specific ATM depletion attenuates the establishment of MHV68 latency

Macrophages are the primary reservoir for latent virus in the peritoneum, whereas B cells harbor the majority of MHV68 in the spleen during the establishment of viral latency (Weck et al., 1999b; Coleman et al., 2010; Collins et al., 2009; Weck et al., 1999a). We previously showed that MHV68 reactivation was 50-fold higher in the peritoneum of ATM deficient mice as compared to wild type littermates (Kulinski et al., 2012). However, ATM deficiency also led to a suboptimal MHV68-specific T cell response that likely masked any infected cell-intrinsic functions of ATM. To determine whether ATM expression within myeloid cells regulated the establishment of MHV68 latency *in vivo*, MHV68 latency and reactivation were assessed in M-Cre positive and negative mice. Due to the mixed genetic background, littermates were directly compared in every experiment.

M-Cre positive mice demonstrated decreased MHV68 reactivation from the peritoneal cells at 20 days post intranasal infection (Fig. 2A, $p=0.02$). This decreased reactivation was not due to decreased viral spread to the peritoneum, as similar frequency of MHV68 genome positive cells was observed in peritoneal cells harvested from M-Cre positive and negative groups (Fig. 2B). Further, decreased frequencies of MHV68 reactivation and MHV68 genome positive cells were observed in M-Cre positive peritoneal cells at 16 days following intraperitoneal inoculation (Fig. 2E, F; $p=0.002$).

Because B cells host a majority of latent MHV68 in the spleen, myeloid-specific ATM deficiency was not expected to alter splenic infection. Indeed, in contrast to decreased virus reactivation in the peritoneum of M-Cre positive mice, similar levels of *ex vivo* reactivation were observed in M-Cre positive and negative splenocytes (Fig. 2C), along with comparable frequencies of MHV68 genome positive splenocytes in these two groups (Fig. 2D). Thus, ATM deficiency limited to myeloid cells attenuated the establishment of MHV68 latency in the peritoneum, but not spleen.

ATM deficiency restricted to myeloid cells fails to alter the MHV68-specific T cell response

In contrast to a 50-fold increase in MHV68 reactivation observed in the peritoneum of ATM deficient mice (Kulinski et al., 2012), myeloid cell-specific ATM deficiency decreased MHV68 reactivation from peritoneal cells (Fig. 2), suggesting that a suboptimal immune response is likely responsible for increased MHV68 reactivation in the peritoneum of mice with global ATM deficiency (Kulinski et al., 2012). Given the importance of the adaptive immune response in controlling MHV68 reactivation (Braaten et al., 2005; Tibbetts et al., 2002; Gredmark-Russ et al., 2008; Ehtisham et al., 1993), parameters of global and MHV68-specific immune responses were examined in M-Cre positive and negative littermates. MHV68 infection induced similar changes in the absolute cell numbers of $CD8^{+}$ and $CD4^{+}$ T cells, B cells, and NK cells in the peritoneum and spleen of M-Cre positive and negative mice (Fig. 3A, B), indicating that myeloid-specific ATM deficiency had no effect on the global cellular immune responses to MHV68 infection.

Next, MHV68-specific $CD8^{+}$ T cell responses were assessed. The first wave of MHV68-specific splenic $CD8^{+}$ T cells (represented by the immunodominant $ORF6_{487-495}$-specific response) expresses early in infection and rapidly declines following clearance of acute replication. The second wave of $CD8^{+}$ T cells

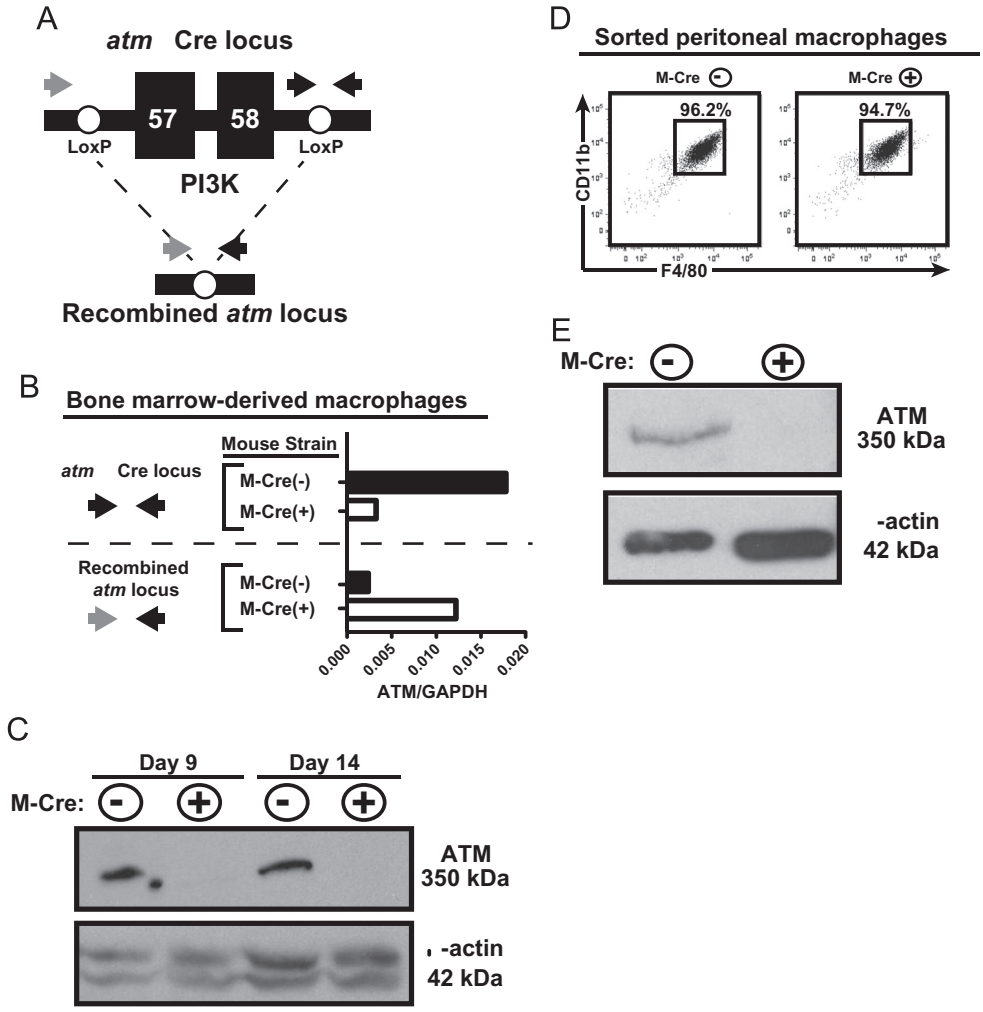

Fig. 1. Validation of M-Cre ATM$^{c/c}$ mouse model. (A) Conditional ATM alleles (ATM$^{c/c}$) include LoxP sequences flanking exons 57 and 58 (PI3K domain of ATM). Cre-mediated recombination results in deletion of exons 57 and 58. Arrows indicate the location of primers used in panel B. (B, C) Bone marrow derived macrophages were generated from M-Cre positive and M-Cre negative mice. (B) Following 14 days of culture, relative abundance of intact and recombined *atm* alleles was measured by qPCR analysis using primers shown in panel A. (C) Whole cell lysates were collected at day 9 and day 14 of culture and ATM and β-actin protein expression assessed by western blot analysis. (D, E) Peritoneal cells were harvested from M-Cre positive or M-Cre negative mice and CD11c$^-$CD11b$^+$F4/80$^+$ cells sorted by FACS. Sorted cells were either analyzed for surface protein expression by flow cytometry (D) or subjected to western blot analysis using indicated antibodies (E).

(represented by the ORF61$_{524–531}$ response) continues to expand throughout early latency in a manner that is dependent upon continued antigenic stimulation (Freeman et al., 2010;Gredmark-Russ et al., 2008). Significantly, ATM deficient mice display altered kinetics of these two MHV68-specific CD8$^+$ T cell responses (Kulinski et al., 2012). In contrast, the frequency and absolute number of ORF6$_{487}$/D^b- and ORF61$_{524}$/K^b-specific CD8$^+$ T cells were similar in M-Cre negative and positive mice (Fig. 3C, D, data not shown). Interestingly, in spite of waning ORF6$_{487}$/D^b -specific T cell response in the spleen, response to this viral epitope continued to dominate in the peritoneum, independent of the M-Cre genotype. Further, the MHV68-specific humoral immune response, determined by measuring MHV68-specific immunoglobulin levels, was similar in M-Cre positive and negative mice (Fig. 3E). Thus, myeloid cell-specific ATM deficiency had no effect on the immune responses to MHV68 infection.

Myeloid cell-specific ATM deficiency has no effect on the relative abundance of myeloid cell types in the spleen or peritoneum

Identical global and MHV68-specific immune responses in M-Cre positive and negative mice (Fig. 3) failed to account for the decreased MHV68 infection observed in M-Cre positive peritoneal cells (Fig. 2). In contrast to the well-known role of ATM in the development of T and B cells (Giovannetti et al., 2002; Matei et al., 2006; D'Souza et al., 2011a), the regulation of myeloid cell development by ATM is less understood. Therefore, we wanted to test the hypothesis that myeloid cell-specific ATM deficiency attenuated differentiation and/or homing of myeloid cells to the peritoneum. To test this hypothesis, the frequency of dendritic cells (CD11c$^+$GR-1$^-$), granulocytes (GR-1$^+$CD11c$^-$), and macrophages (CD11c$^-$GR-1$^-$CD11b$^+$F4/80$^+$) was measured in M-Cre positive and negative littermates under baseline conditions or following MHV68 infection (representative flow plots shown in Fig. 4A). The frequency and absolute number of peritoneal dendritic cells, granulocytes, and macrophages were similar in M-Cre positive and negative mice, both at baseline and following MHV68 infection (Fig. 4B). Interestingly, MHV68 infection resulted in an increased frequency and absolute number of peritoneal GR-1$^+$ granulocytes; however, this increase was independent of the M-Cre genotype (Fig. 4B). Furthermore, a similar increase in surface expression of MHC class I and II was observed in peritoneal macrophages and dendritic cells in response to MHV68 infection, regardless of the M-Cre genotype (data not shown). Thus, myeloid cell-specific ATM depletion did not affect the recruitment of

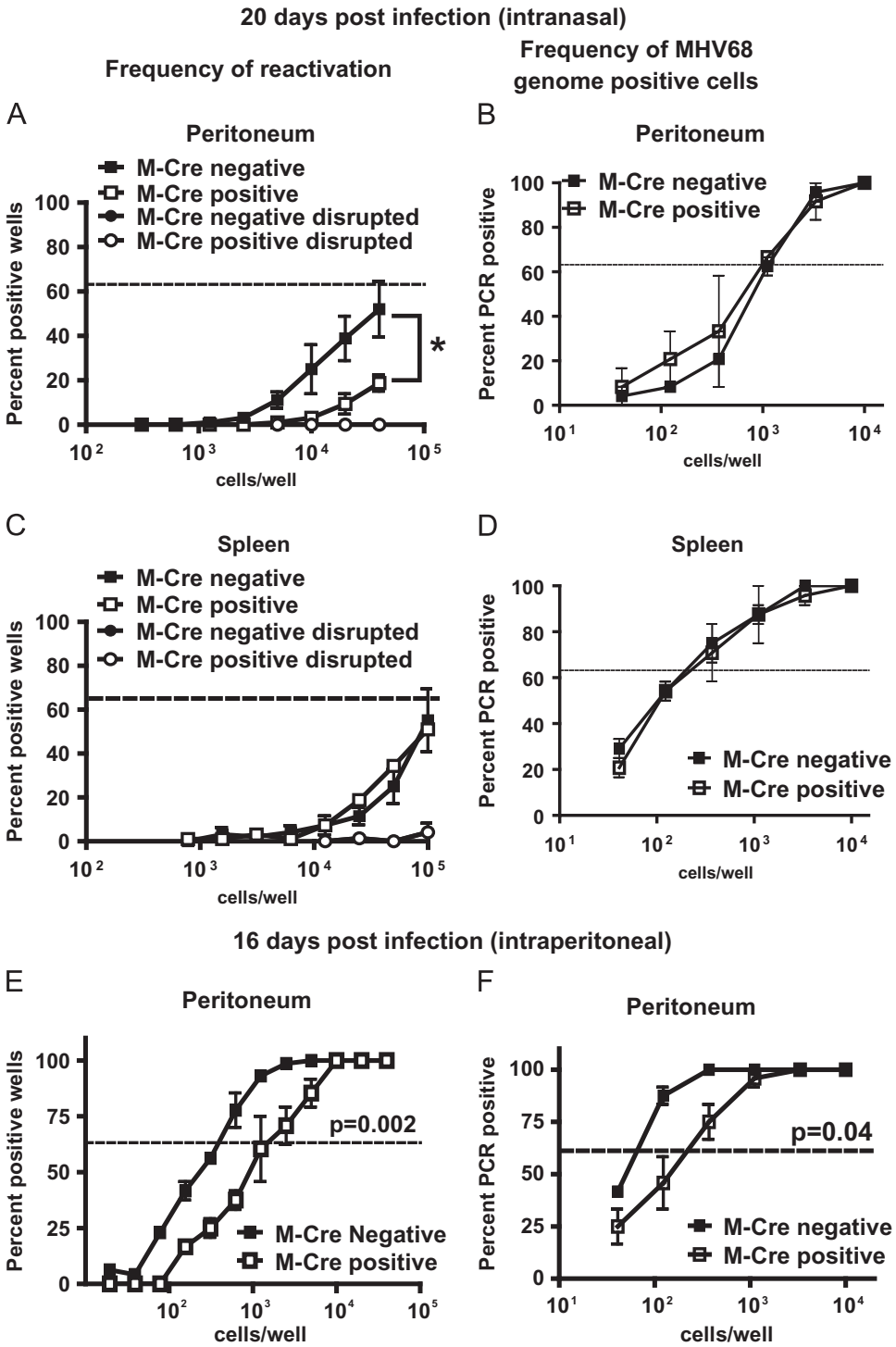

Fig. 2. Myeloid cell-specific ATM depletion attenuates establishment of MHV68 latency. M-Cre positive and negative littermates (3–5 mice/group for each experiment) were intranasally (A–D) or intraperitoneally (E, F) inoculated with 10^4 PFU of MHV68. Splenocytes and peritoneal cells were harvested at 20 (A–D) or 16 (E, F) days post infection and pooled from mice in each experimental group. Frequencies of reactivation (A, C, E) and MHV68-infected cells (B, D, F) were determined using limiting dilution assays. Data were pooled from 2–5 independent experiments and subjected to statistical analyses.

dendritic cell, granulocyte, and macrophage populations to the peritoneum.

Induction of the DNA damage response contributes to viral DNA synthesis during MHV68 reactivation from myeloid cells

Attenuated MHV68 reactivation seen in the peritoneum of M-cre positive mice (Fig. 2) could not be attributed to the inadequate presence of myeloid cells (Fig. 4). Because ATM activity supports reactivation of EBV from latently infected cancer cell lines *in vitro* (Hagemeier et al., 2012a), we examined the effect of acute activation or inhibition of ATM on MHV68 reactivation from peritoneal macrophages.

Generation of double-stranded DNA breaks by γ-irradiation induces a robust activation of ATM in the context of DNA damage response. To determine the effect of DNA damage response on

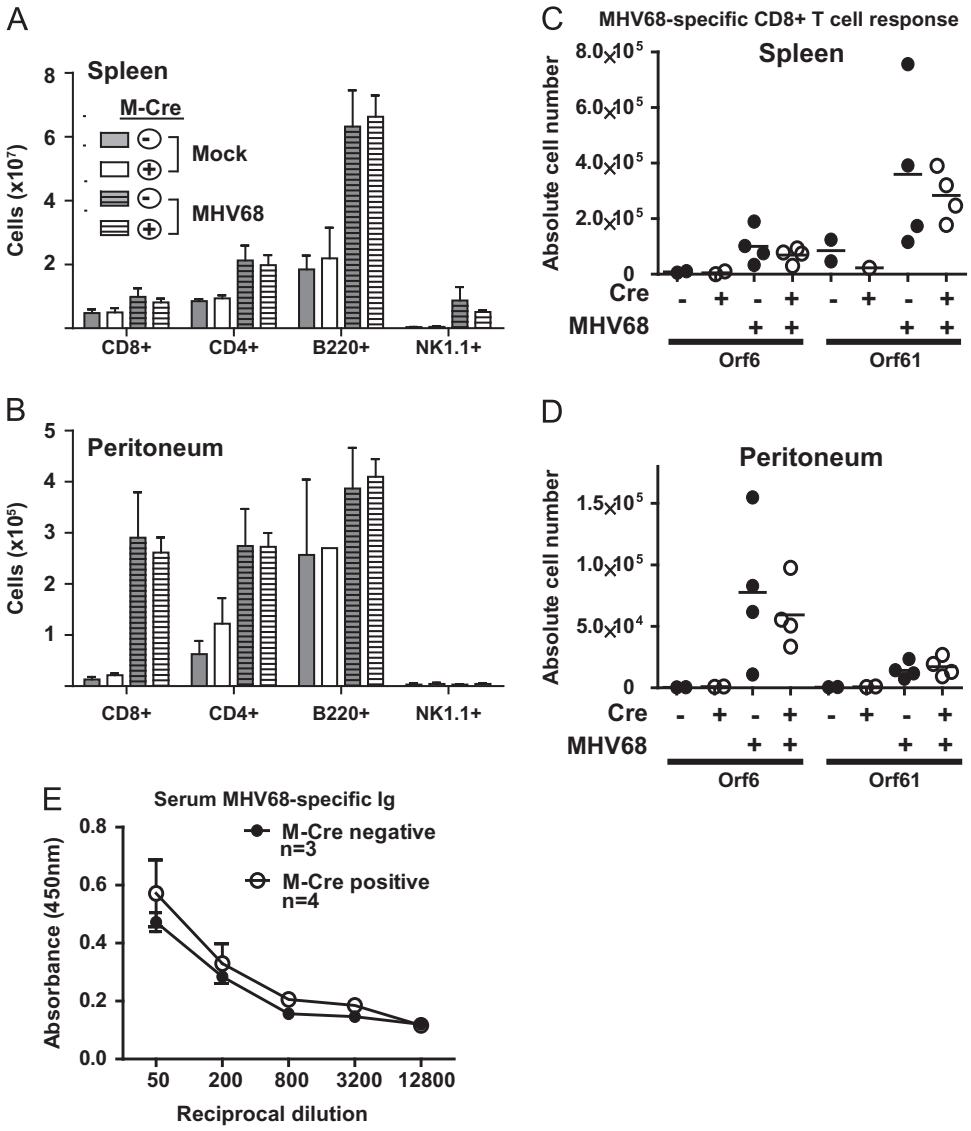

Fig. 3. Myeloid-restricted ATM depletion does not affect MHV68-specific immune response. M-Cre positive or negative littermates were mock-inoculated or intranasally infected with MHV68 as described in Fig. 2. (A, B) Splenocytes and peritoneal cells were harvested at 16–20 days post infection and stained with either anti-CD8 or anti-CD4 in combination with anti-CD3 or with anti-B220 or anti-NK1.1. Data show the absolute number of $B220^+$, $NK1.1^+$, $CD3^+CD8^+$ double positive, and $CD3^+CD4^+$ double positive cells. (C, D) Splenocytes or peritoneal cells harvested from MHV68- or mock-infected mice of indicated genotypes were stained with anti-CD8 and anti-CD3 in combination with either $ORF6_{487}/D^b$ or $ORF61_{524}/K^b$ MHC class I tetramers. Data were pooled from at least 2–3 independent experiments. Floating bars represent the mean and each symbol represents an individual mouse. (E) Serum was collected at 16 days post infection and serial dilutions assayed for MHV68-specific immunoglobulin.

MHV68 reactivation from latently infected macrophages, peritoneal cells were harvested from MHV68-infected BL6 mice, mock- or γ-irradiated upon explantation, and allowed to reactivate the virus. Irradiated cultures demonstrated a dose-dependent increase in the accumulation of MHV68 DNA during reactivation (Fig. 5A), indicating that activation of DNA damage response facilitated viral DNA synthesis during viral reactivation from latently infected peritoneal cells. Because only a small proportion of latently infected peritoneal cells reactivates virus *ex vivo*, this ~3-fold increase in total viral DNA likely reflects a significantly higher increase in DNA synthesis in a subpopulation of infected cells that was reactivating virus. Interestingly, the frequency of *ex vivo* reactivation was not affected by γ-irradiation (Fig. 5B), suggesting that the activation of DNA damage response was not sufficient to initiate *de novo* reactivation of MHV68 from latently infected peritoneal macrophages. Instead, DNA damage response supported viral DNA synthesis in myeloid cells that were already poised to reactivate the virus.

To define the extent to which observed effects of γ-irradiation on MHV68 reactivation were ATM dependent, explanted peritoneal cells were treated with a selective ATM inhibitor (KU-55933) immediately following explantation, irradiated, and levels of viral DNA examined at 24 h post irradiation. The potentiating effect of γ-irradiation on the MHV68 DNA synthesis was lost in KU-55933-treated PEC (Fig. 5C), indicating that the enzymatic activity of ATM is required for the DNA damage response-mediated increase in MHV68 DNA accumulation during reactivation.

ATM expression attenuates levels of reactive oxygen species in MHV68-infected macrophages

Reactive oxygen species (ROS) enhance the expression of immediate early viral genes in EBV- or KSHV-infected cell lines (Lassoued et al., 2010; Li et al., 2011;Ye et al., 2011). Further, ATM can undergo alternative activation in response to ROS (Guo et al.,

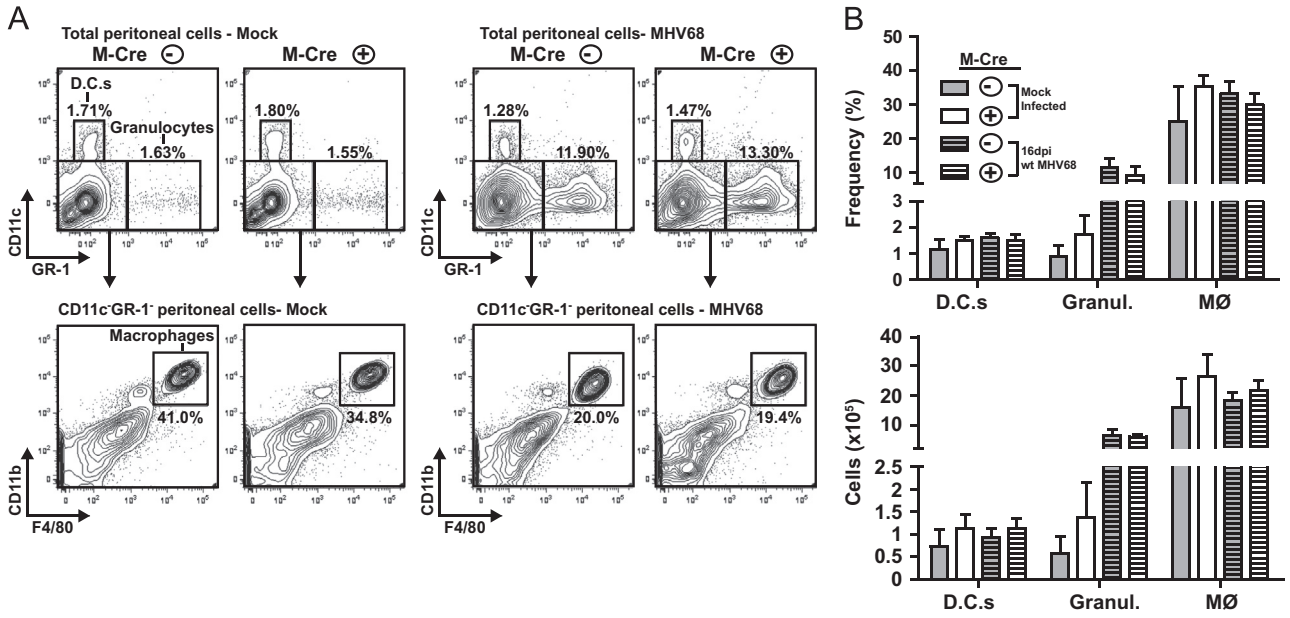

Fig. 4. Myeloid cell-specific ATM deficiency fails to alter relative abundance of myeloid cell types in the peritoneum. M-Cre positive or negative littermates were intranasally infected with MHV68 as in Fig. 2. Peritoneal cells were harvested at 16–20 days post infection and stained with antibodies against CD11c, GR-1, CD11b, and F4/80 for analysis by flow cytometry. (A) Representative flow cytometry plots showing gating strategy in all experimental groups. (B) Absolute number and frequency of indicated myeloid cells populations defined based on the gating strategy shown in panel A. Data were pooled from 2–3 independent experiments, 3–4 mice/group. Error bars represent SEM.

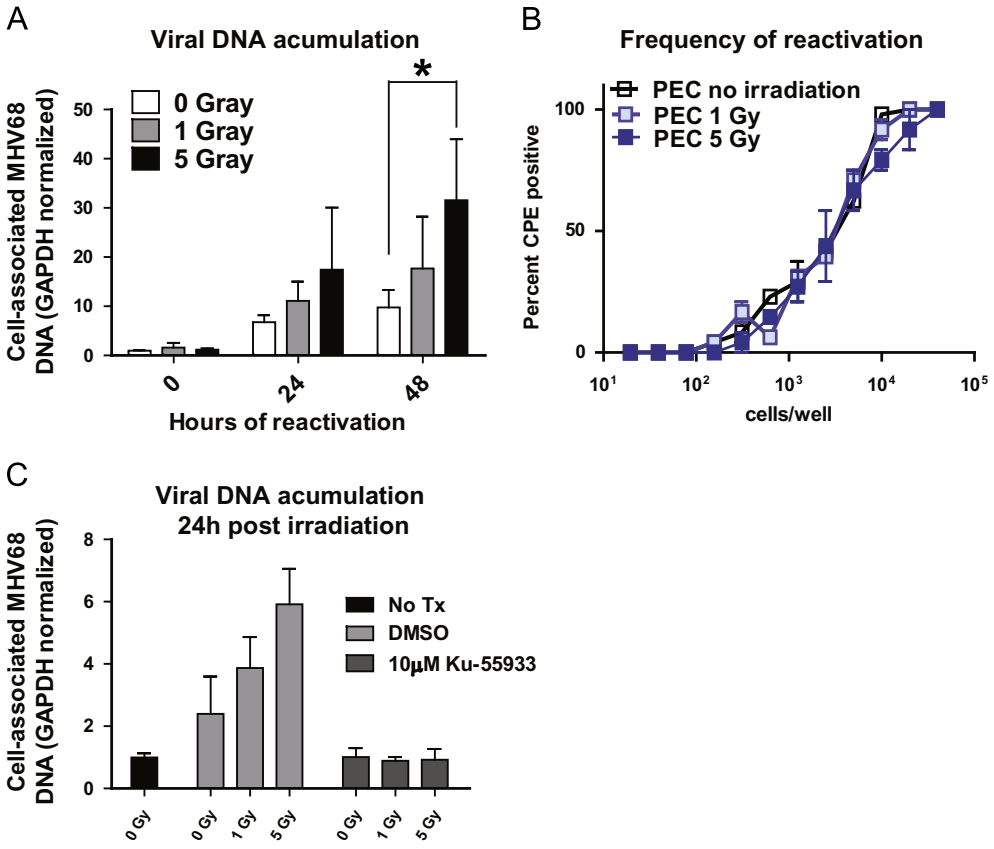

Fig. 5. Induction of the DNA damage response stimulates MHV68 reactivation from latency in an ATM-dependent manner. Peritoneal cells were harvested from BL6 mice infected with MHV68 for 28 days. Following harvest, cells were subjected to indicated doses of γ-irradiation, and allowed to reactivate MHV68 *ex vivo* in untreated medium (A, B, No Tx group in C), or medium supplemented with 10 μM Ku-55933 or DMSO (C). (A, C) Cell-associated DNA was isolated at indicated times post irradiation and viral DNA measured by qPCR with subsequent normalization to cellular GAPDH. To facilitate pooling of data from multiple experiments, in (A), GAPDH-normalized viral DNA levels measured at 24 and 48 h post irradiation were further normalized to those observed in mock-irradiated cells at 0 h of reactivation (set to 1). Similarly, in (C), where only a single time point was examined (24 h post irradiation), viral DNA levels in unirradiated untreated virus-reactivating cultures were set to 1, and the rest of experimental conditions normalized to that value. (B) Frequency of MHV68 reactivation was measured using limiting dilution assay. Data were pooled from 2–3 independent experiments. $^{*}p < 0.05$.

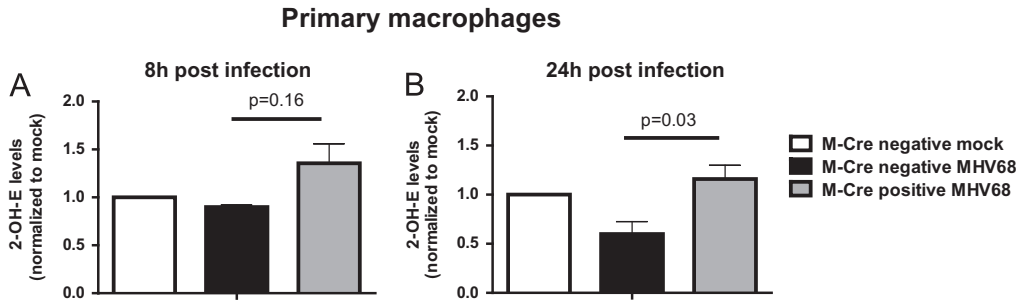

Fig. 6. ATM expression attenuates levels of reactive oxygen species in MHV68-infected macrophages. M-Cre positive and negative primary macrophages were derived from bone marrow of littermates. Macrophages were infected at an MOI of 10 or mock-treated. Hydroethidine (HE) was added at 7 or 23 h post infection at 10 μM. Macrophages were harvested at 8 (A) or 24 (B) hours post infection and superoxide determined by measuring levels of 2-hydroxyethidium (2-OH-E^+) using HPLC. 2-OH-E^+ levels were normalized to protein levels for each sample. Finally, baseline levels observed in mock-infected control macrophages were set at 1 for each examined time point, and the rest of experimental samples within a particular time point normalized to the corresponding mock. Data were pooled from 2–3 independent experiments.

2010), and ATM deficiency is associated with increased ROS levels and oxidative stress *in vivo* (Barlow et al., 1999; Ito et al., 2007). Because less than 1% of all peritoneal exudate cells are MHV68-infected, we have employed an *in vitro* approach to measure the effect of ATM expression on ROS levels specifically in MHV68-infected macrophages.

To define ROS levels during MHV68 infection, primary macrophages were derived from bone marrow of M-Cre negative or M-Cre positive littermates (Fig. 1B, C). Macrophages were infected at a high multiplicity of infection and oxidative stress was determined by measuring superoxide formation by following oxidation of hydroethidine to 2-hydroxyethidium (2-OH-E^+) (Kalyanaraman et al., 2012). At 8 h post infection (early stage of infection, prior to viral DNA synthesis), similar levels of superoxide were detected in M-Cre negative and positive infected macrophages (Fig. 6A). Interestingly, by 24 h post infection, superoxide levels were about 2-fold lower in MHV68-infected control macrophages as compared to infected M-Cre positive cultures (Fig. 6B). Thus, ATM expression decreased ROS levels in MHV68-infected primary macrophages at late, but not early stages of viral replication.

Myeloid cell-specific ATM deficiency does not attenuate MHV68 long-term latency

Between 16 and 42 days post infection MHV68 transitions from early latency to a stable long term condition with a decrease and subsequent stabilization of the latent reservoir and an attenuation of *ex vivo* reactivation. Because MHV68 infection was decreased in M-Cre positive peritoneal cells during the establishment of viral latency (Fig. 2), effects of myeloid cell-specific ATM deficiency on long-term latency were examined. The frequencies of MHV68 genome positive splenocytes and peritoneal cells were similar in M-cre positive and negative mice at 42 days post infection (Fig. 7C, D), with very little virus reactivation present in the spleens of either genotype (Fig. 7B). Surprisingly, the frequency of MHV68 reactivation was also similar in the peritoneal cells of M-cre positive and negative mice (Fig. 7A).

One possible explanation for these results was that Cre expression was suppressed in older mice, leading to restored ATM expression in M-Cre positive peritoneal macrophages. To test this possibility, ATM protein levels were measured in macrophages ($CD11b^+F4/80^+$) and non-myeloid ($CD11b^-F4/80^-$) peritoneal cells sorted from M-Cre positive animals at 42 days post MHV68 infection (Fig. 7E). ATM protein expression remained below the level of detection in M-Cre positive peritoneal macrophages, while ATM expression was maintained in non-myeloid peritoneal cells (Fig. 7F), suggesting that functional Cre was expressed in myeloid cells throughout the 42 days of infection. Thus, myeloid-cell specific ATM deficiency did not attenuate long-term MHV68 infection.

Discussion

To our knowledge, this study provides the first evidence that ATM facilitates gammaherpesvirus reactivation *in vivo*, in the context of chronic infection of a natural host. Based on our published (Kulinski et al., 2012) and current studies, we would like to propose the following working model (Fig. 7G). ATM regulates the establishment of chronic gammaherpesvirus infection via two opposing functions. On one hand, antiviral function of ATM facilitates the development of MHV68-specific adaptive immune response that suppresses viral reactivation. This antiviral role of ATM is likely to be mediated by T cell-intrinsic functions of ATM. On the other hand, ATM plays a proviral role by facilitating viral reactivation during early MHV68 latency. The antiviral and proviral roles of ATM illustrate a host-virus balance that both limits and allows the establishment of chronic virus infection.

Role of ATM in shaping gammaherpesvirus infection in vivo

A-T patients are susceptible to severe herpesvirus infections and uniformly display high EBV viral loads (Folgori et al., 2010; Lankisch et al., 2013; Masucci et al., 1984; Morio et al., 2009; Nowak-Wegrzyn et al., 2004; Saemundsen et al., 1981; Ben-Zvi et al., 1978), suggesting that ATM is an important host factor that regulates chronic gammaherpesvirus infection. Because ATM deficiency is not associated with universal susceptibility to virus infections, the mechanism by which ATM regulates chronic herpesvirus infection remains poorly understood. Consistent with the clinical presentation in humans, we previously showed that ATM deficient mice display increased MHV68 reactivation and persistent replication, along with an attenuated and altered MHV68-specific CD8 T cell response (Kulinski et al., 2012) that was likely to be responsible for increased viral lytic activity. However, it was not clear whether this altered antiviral immune response was driven by T cell-extrinsic or intrinsic factors. In this study we found that myeloid–specific ATM deficiency had no effect on the development of MHV68-specific CD8 T cell response, suggesting that T cell-intrinsic ATM functions are likely to be important for the development of a proper adaptive immune response against herpesviruses.

Importantly, in the presence of a wild type antiviral immune response, myeloid-specific ATM deficiency attenuated the establishment of MHV68 latency, despite the presence of adequate numbers of macrophages and dendritic cells. These observations suggest that ATM has direct effects in potentiating the

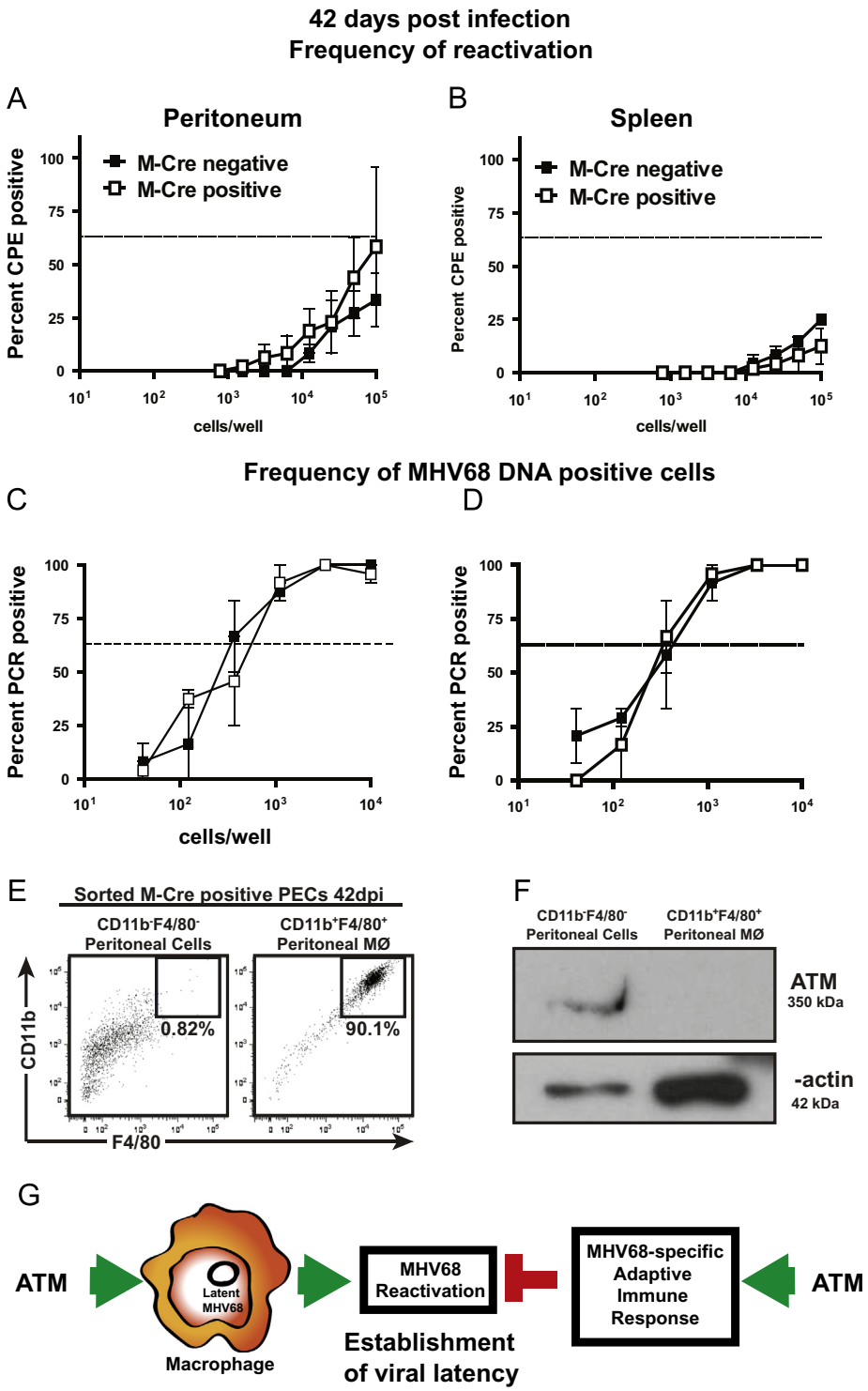

Fig. 7. Effect of myeloid cell-specific ATM deficiency on long-term MHV68 latency. Cre positive or negative littermates were intranasally infected with MHV68 as in Fig. 2. Splenocytes and PEC were harvested at 42 days post infection and pooled from 3–5 mice in each experimental group. Frequency of reactivation (A, B) and MHV68 genome positive cells (C, D) was determined using limiting dilution assays. Data were pooled from 2–3 independent experiments. (E) Representative flow diagram of sorted macrophages and non-macrophage peritoneal cells harvested from M-Cre positive MHV68-infected mice. (F) Western analysis of sorted populations presented in panel C. (G) Working model. A combination of proviral and antiviral functions of ATM balances host-gammaherpesvirus interaction *in vivo*. ATM restricts gammaherpesvirus reactivation by promoting the development of virus-specific adaptive immune response. In parallel, ATM expression within the myeloid cells facilitates gammaherpesvirus reactivation.

establishment of MHV68 latency and viral reactivation from myeloid cells, similar to that observed *in vitro* for EBV and KSHV (Hagemeier et al., 2012a; Singh et al., 2013). Interestingly, the ATM-dependent enhancement of MHV68 reactivation from myeloid cells was limited to early viral latency, and was not evident in long-term infected animals. Our studies excluded the possibility that myeloid-specific Cre function was lost in long term-infected mice (Fig. 7E, F). One obvious interpretation of the

observed phenotype is that MHV68 no longer requires ATM for reactivation during long-term infection; however, a negative result is not definitive. An alternative interpretation is that the MHV68 tropism may be shifting away from the peritoneal macrophages to a different cell type during long-term infection; a cell type that will not be expected to express Cre recombinase. Interestingly, the M-Cre transgene is not efficiently expressed in dendritic cells (Clausen et al., 1999), a cell type that can support MHV68 latency.

Role of ATM in MHV68 reactivation

Results of our study support the model where ATM directly facilitates gammaherpesvirus reactivation in myeloid cells *in vivo*. This proviral role of ATM is consistent with published *in vitro* studies showing that ATM facilitates EBV reactivation from latently infected cancer cell lines (Hagemeier et al., 2012b), supports MHV68 replication in primary macrophages (Tarakanova et al., 2007), and enhances the establishment of KSHV latency in endothelial cells (Singh et al., 2013). Specifically, ATM activity facilitates EBV immediate early lytic gene expression in EBV-positive B cell- and epithelial cell lines following diverse types of reactivation-inducing stimuli (Hagemeier et al., 2012b). The role of ATM in MHV68 immediate early viral gene expression is further supported by our previous work that demonstrated a requirement for H2AX, an ATM substrate, for the optimal expression of MHV68 immediate early gene (Mounce et al., 2011a).

Many stimuli that induce gammaherpesvirus reactivation are associated with an increase in ROS levels (Ye et al., 2011). It has long been recognized that oxidative stress potentiates the expression of immediate early viral genes in both EBV- and KSHV-infected cell lines (Lassoued et al., 2010; Li et al., 2011; Ye et al., 2011). Intriguingly, ROS activate ATM indirectly, via the generation of DNA breaks, and directly, via an alternative oxidation-dependent molecular mechanism (Guo et al., 2010) and ATM is thought to mitigate oxidative stress *in vivo* (Barlow et al., 1999; Ito et al., 2007). We found that ATM deficiency in primary macrophages resulted in a slight increase (~2-fold) in ROS levels at late, but not early stages of MHV68 infection (Fig. 6). However, these increased ROS levels in ATM deficient cells do not translate into increased MHV68 replication; instead MHV68 replication is attenuated in ATM deficient macrophages (Tarakanova et al., 2007). A challenge for future studies will be to reconcile the role of ATM in oxidative stress with its other functions to establish a mechanistic understanding of how ATM and its substrates support gammaherpesvirus lytic gene expression and DNA synthesis during reactivation.

In summary, the results of this and other studies support a working model where ATM opposes gammaherpesvirus infection by facilitating the development of a gammaherpesvirus-specific T cell response, and is simultaneously usurped by the virus to enhance viral reactivation. This balance of proviral and antiviral activities of ATM may be further regulated by the emerging alternative functions of ATM outside of DNA damage response, including its role in insulin signaling and metabolic pathways (Shiloh and Ziv, 2013).

Conclusions

A majority of adults worldwide are permanently infected with gammaherpesviruses, a family of viruses that is associated with several types of cancer. However, only a proportion of infected individuals will develop gammaherpesvirus-induced cancer, necessitating identification of host factors that regulate chronic gammaherpesvirus infection. Our previous work showed that global deficiency of Ataxia-Telangiectasia mutated (ATM) kinase leads to a poor control of chronic gammaherpesvirus infection along with an altered virus-specific immune response, underscoring the antiviral role of ATM. In this study myeloid cell-specific deficiency of ATM attenuated the establishment of gammaherpesvirus latency *in vivo*, uncovering a proviral function of ATM. Thus, we propose that ATM combines both anti- and proviral activities to balance host-gammaherpesvirus interaction during chronic infection *in vivo*.

Materials and methods

Mice

All mice were housed and bred in a specific pathogen free barrier facility in accordance with federal and institutional guidelines. All experimental manipulations of mice were approved by the Institutional Animal Care and Use Committee of the Medical College of Wisconsin (AUA971). C57BL/6 J and M-Cre (B6.129P2-*Lyz2*$^{tm1(cre)Ifo}$/J) mice were originally obtained from Jackson Laboratories (Bar Harbor, ME). ATM flox (ATM$^{c/c}$) mice were a kind gift from Dr. Fred Alt (HHMI, Harvard Medical School). A combination of ATMgF86723 (5′ ATC AAA TGT AAA GGC GGC TTC 3′), BAC13 (5′ CAT CCT TTA ATG TGC CTC CCT TCG CC 3′), and BAC 7 (5′ GCC CAT CCC GTC CAC AAT ATC TCT GC 3′) primers were used to detect either the floxed AtmΔcre (420 bp- floxed, 350 bp-wild type) or the recombined AtmDel allele (903 bp) (Zha et al., 2008) in ATM$^{c/c}$ mice using a strategy outlined in Fig. 1. Cre transgene was detected in the parental B6.129P2-*Lyz2*$^{tm1(cre)Ifo}$/J and M-Cre ATM$^{c/c}$ mice using primers 483 (5′ CGA TGC AAC GAG TGA TGA GG 3′) and 770 (5′ GCA TTG CTG TCA CT TGGT CGT 3′)(280 bp).

Virus infections in vivo

Wild type MHV68 virus stock was prepared and titered on NIH 3T12 cells as previously described (Mounce et al., 2011b). Due to the mixed genetic background of the M-Cre mouse strain, Cre positive and negative littermates were directly compared. In each experiment, 3–5 mice/genotype were infected. Specifically, infections were performed by intranasal or intraperitoneal inoculation at 6–7 weeks of age with 10^4 plaque forming units of MHV68 or sterile carrier in an inoculum volume of 15 μl (intranasal) or 200 μl (intraperitoneal) per mouse. Virus was diluted in sterile serum-free Dulbecco's modified Eagle's medium (Corning, Tewksbury, MA). Upon termination of the experiment, splenocytes, peritoneal cells, and serum were collected from each mouse. In viral latency experiments, splenocytes and peritoneal cells were pooled from all mice of the same genotype. These pooled cell suspensions (splenocytes or peritoneal exudate cells) were subjected to limiting dilution assays as described below. Pooled peritoneal cells were also subjected to flow cytometry-based sorting and ex vivo reactivation experiments. In contrast, splenocytes and peritoneal cells harvested from individual mice were analyzed as individual samples by flow cytometry and ELISA.

Tissue culture

NIH 3T12 cells were maintained in Dulbecco's modified Eagle's medium supplemented with 10% fetal bovine serum, 100 U/ml penicillin, 100 mg/ml streptomycin, and 2 mM L-glutamine. Mouse embryonic fibroblasts were maintained in Dulbecco's modified Eagle's medium supplemented with 10% fetal calf serum, 25 U/ml penicillin, 25 mg/ml streptomycin, 2.6 mM L-glutamine, and non-essential amino acids. Bone marrow derived macrophages were generated as previously described (Tarakanova et al., 2007).

Flow cytometry

Single cell suspensions were resuspended in FACS buffer (PBS+2% FCS+0.05% sodium azide) at 1×10^7 cells/ml. A total of 1×10^6 cells were prestained with Fc block (24G2), then incubated with an optimal amount of antibody conjugate (eFluor450, fluorescein isothiocyanate, r-phycoerythrin, PE-Cy7, or allophycocyanin). Antibodies to the following molecules were purchased from eBioscience (San Diego, CA): B220/CD45R (RA3–6B2), CD8a/Ly-2 (53–6.7), CD4 (RM4–5), MHC-I (28–14–8), MHC-II (25–9–17), CD11b (M1/70), CD11c (N418), GR-1 (RB6-8C5), F4/80 (BM8). Data acquisition was performed on a LSR II flow cytometer (BD Biosciences, Sparks, MD) and analyzed using FlowJo software (Tree Star, Ashland, OR). MHV68 tetramers were provided by the NIH Tetramer Core Facility.

Cell sorting

Single cell suspensions of PEC were stained with anti-CD11c, anti-CD11b and anti-F4/80 as described above for flow cytometry analysis, and $CD11c^-CD11b^+F4/80^+$ and $CD11c^-CD11b^-F4/80^-$ fractions isolated using a FACSAria cell sorter (Becton Dickinson, San Jose, CA). Sorted cells were subsequently analyzed by flow cytometry for purity.

MHV68-specific Ig assays

Nunc Maxisorp immunoplates (Fisher Scientific, Pittsburgh, PA) were coated overnight at 4 °C with UV-irradiated MHV68 virus stock (740,000 microjoules/$cm^2 \times 2$; Stratalinker UV Crosslinker 1800 - Agilent Technologies, Santa Clara, CA). Plates were washed five times with PBS-Tween (0.05%), blocked for 1 h with PBS-Tween (0.05%)-bovine serum albumin (3%, Fisher Scientific), incubated with serial 3-fold dilutions of experimental serum in PBS-Tween (0.05%)-bovine serum albumin (0.5%) for 1 h, and washed five times. Bound antibody was detected with horse radish peroxidase-conjugated goat anti-mouse IgM and goat anti-mouse IgG (heavy+light chain) (all from Jackson ImmunoResearch, West Grove,PA) using 3,3′, 5,5′-tetramethylbenzidine substrate (Life Technologies, Gaithersburg, MD). HRP enzymatic activity was stopped by the addition of 1 N HCL (Sigma-Aldrich, St. Louis, MO) and the absorbance read at 450 nm on a model 1420 Victor^{3}V Multilabel Plate Reader (PerkinElmer, Waltham, MA).

Western blot analysis

Samples were collected in laemmli buffer (0.1 M Tris 4% SDS, 4 mM EDTA, 100 mM betamercaptoethanol, 3.2 M glycerol with 0.05% bromophenol blue), boiled for 10 min, and subjected to SDS–PAGE. The protein was transferred to a polyvinylidene difluoride membrane (Immunobilon from Millipore, Billerica, MA) using a Transblot transfer cell semi-dry system (Bio-Rad, Hercules, CA). Membranes were blocked overnight with 5% ovalbumin in TBST buffer (150 mM NaCl, 10 mM Tris, and 0.2% Tween) at 4 °C. Proteins were visualized with a rabbit anti-ATM monoclonal antibody (1:500, Clone D2E2, Cell Signaling Technology, Boston MA) or an anti-β-actin antibody (1:15,000; clone AC-74, Novus Biologicals, Littleton, CO) followed by secondary HRP-conjugated antibodies (1:20,000, Jackson Immunoresearch, West Grove, Pennsylvania).

Limiting dilution analysis

Limiting dilution *ex vivo* reactivation and nested PCR analyses were performed as previously described to measure the frequency of cells reactivating MHV68 or harboring the MHV68 genome, respectively (Tarakanova et al., 2010).

Ex vivo irradiation and quantitation of viral DNA

Peritoneal cells were harvested and pooled from 3–5 MHV68-infected C57BL/6 J mice in each experiment. For experiments presented in Fig. 5C, PEC were plated in DMEM supplemented with 10 μM KU-55933 (Chemdea, Ridgewood NJ) or dimethyl sulfoxide and incubated at 37 °C, 5%CO_2 for 2 h. Peritoneal cells either pre-incubated as above (Fig. 5C) or directly ex vivo (Fig. 5A) were subsequently subjected to 0 (control), 1, or 5 Gy of γ-irradiation; 0 Gy cultures were transported and handled identical to irradiated cultures minus the irradiation. Total DNA was extracted immediately (0 h, Fig. 5A) or after incubation at 37 °C, 5% CO_2 for 24 (Fig. 5A, C) or 48 h (Fig. 5A) following irradiation by the addition of the lysis buffer (0.75% SDS, 40 μg/ml proteinase K, 10 mM Tris–HCl pH 8.1, 1 mM EDTA). Samples were incubated overnight at 56 °C,extracted twice with phenol/chloroform and once with chloroform. DNA was precipitated from the aqueous phase and resuspended in TE buffer (10 mM Tris–HCl pH 8.1, 1 mM EDTA). Viral DNA was quantified using the iQ5 Real-Time PCR detection system (Bio-Rad Laboratories, Hercules, CA) with gene 50- and GAPDH-specific primers (Tarakanova et al., 2010), and normalized values calculated by the ΔC_T method.

Oxidative stress measurements

Oxidation of hydroethidine (HE, Molecular Probes) to 2-hydroxyethidium (2-OH-E^+) was used as an indicator of superoxide production in bone marrow-derived macrophages using a previously described method (Zielonka et al., 2009). Briefly, macrophages were mock infected or infected with MHV68 for 8 h or 24 h and HE (10 μM) was added for the last hour of incubation. The cells were then washed twice with ice-cold PBS and the plates were frozen at −80 °C. Next day, the cells were scraped into 60 μl DPBS containing 0.1% Triton-X100. Two wells were pooled together and samples were syringe-lysed. Subsequently, 80 μl of lysate was mixed with 80 μL of 0.2 M $HClO_4$ in methanol to extract oxidation products of HE. Samples were incubated on ice for 1 h, followed by centrifugation (16000*g* for 15 min, 4 °C). Resulting supernatant (80 μl) was mixed with 1 M potassium phosphate, pH 2.6 (80 μl). Samples were centrifuged and supernatants were analyzed by HPLC using Shimadzu Prominence system equipped with UV/Vis and fluorescent detectors. The analysis was performed on Kinetex C18 column (100 × 4.6 mm, 2.6 μm, Phenomenex, Torrance, CA) as previously described (Broniowska et al., 2013). For the quantification of the 2-OH-E^+ levels, the peak area detected by the fluorescence detector (ex. 490 nm, em. 567 nm) was used and compared to the known amounts of standard. 2-OH-E^+ levels were further normalized to the protein levels in each sample.

Acknowledgment

Expert technical assistance was provided by Chelsea Spurley and Michaela Rekow. We are grateful to Fred Alt for his generous gift of ATM conditional mice. We thank Mike Korrer, Kristen Barr, and Mika Nagaoka for helpful discussions. This study was funded by the American Cancer Society Research Scholar Grant RSG-12–174-01-MPC, R01CA183593-01A1, Wisconsin Breast Cancer Showhouse (V.L.T.), and 1F31CA177279-01 (B.C.M.).

References

Barlow, C., Dennery, P.A., Shigenaga, M.K., Smith, M.A., Morrow, J.D., Roberts, L.J., Wynshaw-Boris, A., Levine, R.L., 1999. Loss of the ataxia-telangiectasia gene

product causes oxidative damage in target organs. Proc. Natl. Acad. Sci. U. S. A. 96, 9915–9919.
Ben-Zvi, A., Soffer, D., Yatziv, S., 1978. Disseminated Herpes simplex virus infection in ataxia-telangiectasia. Acta Paediatr. Scand. 67, 667–670.
Braaten, D.C., Sparks-Thissen, R.L., Kreher, S., Speck, S.H., Virgin, H.W., 2005. An optimized CD8+ T-cell response controls productive and latent gammaherpesvirus infection. J. Virol. 79, 2573–2583.
Broniowska, K.A., Diers, A.R., Corbett, J.A., Hogg, N., 2013. Effect of nitric oxide on naphthoquinone toxicity in endothelial cells: role of bioenergetic dysfunction and poly (ADP-ribose) polymerase activation. Biochemistry 52, 4364–4372.
Campbell, T.B., Borok, M., Gwanzura, L., MaWhinney, S., White, I.E., Ndemera, B., Gudza, I., Fitzpatrick, L., Schooley, R.T., 2000. Relationship of human herpesvirus 8 peripheral blood virus load and Kaposi's sarcoma clinical stage. AIDS 14, 2109–2116.
Cesarman, E., 2011. Gammaherpesvirus and lymphoproliferative disorders in immunocompromised patients. Cancer Lett. 305, 163–174.
Clausen, B.E., Burkhardt, C., Reith, W., Renkawitz, R., Forster, I., 1999. Conditional gene targeting in macrophages and granulocytes using LysMcre mice. Transgenic Res. 8, 265–277.
Coleman, C.B., Nealy, M.S., Tibbetts, S.A., 2010. Immature and transitional B cells are latency reservoirs for a gammaherpesvirus. J. Virol. 84, 13045–13052.
Collins, C.M., Boss, J.M., Speck, S.H., 2009. Identification of infected B-cell populations by using a recombinant murine gammaherpesvirus 68 expressing a fluorescent protein. J. Virol. 83, 6484–6493.
D'Souza, A.D., Parish, I.A., McKay, S.E., Kaech, S.M., Shadel, G.S., 2011a. Aberrant CD8 T-cell responses and memory differentiation upon viral infection of an ataxia-telangiectasia mouse model driven by hyper-activated Akt and mTORC1 signaling. Am. J. Pathol. 178, 2740–2751.
D'Souza, A.D., Parish, I.A., McKay, S.E., Kaech, S.M., Shadel, G.S., 2011b. Aberrant CD8+ T-cell responses and memory differentiation upon viral infection of an ataxia-telangiectasia mouse model driven by hyper-activated Akt and mTORC1 signaling. Am. J. Pathol. 178, 2740–2751.
Efstathiou, S., Ho, Y.M., Hall, S., Styles, C.J., Scott, S.D., Gompels, U.A., 1990. Murine herpesvirus 68 is genetically related to the gammaherpesviruses Epstein–Barr virus and herpesvirus saimiri. J. Gen. Virol. 71, 1365–1372.
Ehtisham, S., Sunil- Chandra, N.P., Nash, A.A., 1993. Pathogenesis of murine gammaherpesvirus infection in mice deficient in CD4 and CD8 T cells. J. Virol. 67, 5247–5252.
Feng, W.H., Cohen, J.I., Fischer, S., Li, L., Sneller, M., Goldbach-Mansky, R., Raab-Traub, N., Delecluse, H.J., Kenney, S.C., 2004. Reactivation of latent Epstein–Barr virus by methotrexate: a potential contributor to methotrexate-associated lymphomas. J. Natl. Cancer Inst. 96, 1691–1702.
Folgori, L., Scarselli, A., Angelino, G., Ferrari, F., Antoccia, A., Chessa, L., Finocchi, A., 2010. Cutaneous granulomatosis and combined immunodeficiency revealing Ataxia-Telangiectasia: a case report. Ital. J. Pediatr. 36, 29.
Freeman, M.L., Lanzer, K.G., Cookenham, T., Peters, B., Sidney, J., Wu, T.T., Sun, R., Woodland, D.L., Sette, A., Blackman, M.A., 2010. Two kinetic patterns of epitope-specific CD8 T-cell responses following murine gammaherpesvirus 68 infection. J. Virol. 84, 2881–2892.
Giovannetti, A., Mazzetta, F., Caprini, E., Aiuti, A., Marziali, M., Pierdominici, M., Cossarizza, A., Chessa, L., Scala, E., Quinti, I., Russo, G., Fiorilli, M., 2002. Skewed T-cell receptor repertoire, decreased thymic output, and predominance of terminally differentiated T cells in ataxia telangiectasia. Blood 100, 4082–4089.
Gredmark-Russ, S., Cheung, E.J., Isaacson, M.K., Ploegh, H.L., Grotenbreg, G.M., 2008. The CD8 T-cell response against murine gammaherpesvirus 68 is directed toward a broad repertoire of epitopes from both early and late antigens. J. Virol. 82, 12205–12212.
Gregorek, H., Chrzanowska, K.H., Dzierzanowska-Fangrat, K., Wakulinska, A., Pietrucha, B., Zapasnik, A., Zborowska, M., Pac, M., Smolka-Afifi, D., Kasztelewicz, B., Piekutowska-Abramczuk, D., Maldyk, J., 2010. Nijmegen breakage syndrome: long-term monitoring of viral and immunological biomarkers in peripheral blood before development of malignancy. Clin. Immunol. 135, 440–447.
Guo, Z., Kozlov, S., Lavin, M.F., Person, M.D., Paull, T.T., 2010. ATM activation by oxidative stress. Science 330, 517–521.
Hagemeier, S.R., Barlow, E.A., Meng, Q., Kenney, S.C., 2012a. The cellular ataxia telangiectasia-mutated kinase promotes Epstein–Barr virus lytic reactivation in response to multiple different types of lytic reactivation-inducing stimuli. J. Virol. 86, 13360–13370.
Hagemeier, S.R., Barlow, E.A., Meng, Q., Kenney, S.C., 2012b. The cellular ataxia telangiectasia-mutated kinase promotes Epstein–Barr virus lytic reactivation in response to multiple different types of lytic reactivation-inducing stimuli. J. Virol. 86, 13360–13370.
Ito, K., Takubo, K., Arai, F., Satoh, H., Matsuoka, S., Ohmura, M., Naka, K., Azuma, M., Miyamoto, K., Hosokawa, K., Ikeda, Y., Mak, T.W., Suda, T., Hirao, A., 2007. Regulation of reactive oxygen species by Atm is essential for proper response to DNA double-strand breaks in lymphocytes. J. Immunol. 178, 103–110.
Kalyanaraman, B., Darley-Usmar, V., Davies, K.J., Dennery, P.A., Forman, H.J., Grisham, M.B., Mann, G.E., Moore, K., Roberts, L.J., Ischiropoulos, H., 2012. Measuring reactive oxygen and nitrogen species with fluorescent probes: challenges and limitations. Free. Radic. Biol. Med. 52, 1–6.
Kulinski, J.M., Leonardo, S.M., Mounce, B.C., Malherbe, L.P., Gauld, S.B., Tarakanova, V.L., 2012. Ataxia-Telangiectasia mutated kinase controls chronic gammaherpesvirus infection. J. Virol. 86, 12826–12837.
Lankisch, P., Adler, H., Borkhardt, A., 2013. Testing for herpesvirus infection is essential in children with chromosomal-instability syndromes. J. Virol. 87, 3616–3617.
Lassoued, S., Gargouri, B., El Feki, A.F., Attia, H., Van, P.J., 2010. Transcription of the Epstein–Barr virus lytic cycle activator BZLF-1 during oxidative stress induction. Biol. Trace Elem. Res. 137, 13–22.
Lavin, M.F., 2008. Ataxia-telangiectasia: from a rare disorder to a paradigm for cell signalling and cancer. Nat. Rev. Mol. Cell Biol. 9, 759–769.
Li, X., Feng, J., Sun, R., 2011. Oxidative stress induces reactivation of Kaposi's sarcoma-associated herpesvirus and death of primary effusion lymphoma cells. J. Virol. 85, 715–724.
Masucci, G., Berkel, I., Masucci, M.G., Ernberg, I., Szigeti, R., Ersoy, F., Sanal, O., Yegin, O., Henle, G., Henle, W., 1984. Epstein–Barr virus (EBV)-specific cell-mediated and humoral immune responses in ataxia-telangectasia patients. J. Clin. Immunol. 4, 369–382.
Matei, I.R., Guidos, C.J., Danska, J.S., 2006. ATM-dependent DNA damage surveillance in T-cell development and leukemogenesis: the DSB connection. Immunol. Rev. 209, 142–158.
Meerbach, A., Wutzler, P., Hafer, R., Zintl, F., Gruhn, B., 2008. Monitoring of Epstein–Barr virus load after hematopoietic stem cell transplantation for early intervention in post-transplant lymphoproliferative disease. J. Med. Virol. 80, 441–454.
Morio, T., Takahashi, N., Watanabe, F., Honda, F., Sato, M., Takagi, M., Imadome, K.I., Miyawaki, T., Delia, D., Nakamura, K., Gatti, R.A., Mizutani, S., 2009. Phenotypic variations between affected siblings with ataxia-telangiectasia: ataxia-telangiectasia in Japan. Int. J. Hematol. 90, 455–462.
Mounce, B.C., Tsan, F.C., Droit, L., Kohler, S., Cirillo, L.A., Tarakanova, V.L., 2011a. Gammaherpesvirus gene expression and DNA synthesis are facilitated by viral protein kinase and histone variant H2AX. Virology 420, 73–81.
Mounce, B.C., Tsan, F.C., Kohler, S., Cirillo, L.A., Tarakanova, V.L., 2011b. Dynamic association of gammaherpesvirus DNA with core histone during de novo lytic infection of primary cells. Virology 421, 167–172.
Nowak-Wegrzyn, A., Crawford, T.O., Winkelstein, J.A., Carson, K.A., Lederman, H.M., 2004. Immunodeficiency and infections in ataxia-telangiectasia. J. Pediatr. 144, 505–511.
Orlandi, E., Paulli, M., Viglio, A., Pagnucco, G., Riboni, R., Baldanti, F., Lazzarino, M., 2001. Epstein–Barr virus-positive aggressive lymphoma as a consequence of immunosuppression after multiple salvage treatments for follicular lymphoma. Br. J. Haematol. 112, 373–376.
Saemundsen, A.K., Berkel, A.I., Henle, W., Henle, G., Anvret, M., Sanal, O., Ersoy, F., Caglar, M., Klein, G., 1981. Epstein–Barr-virus-carrying lymphoma in a patient with ataxia-telangiectasia. Br. Med. J. (Clin. Res.Ed.) 282, 425–427.
Savitsky, K., Bar-Shira, A., Gilad, S., Rotman, G., Ziv, Y., Vanagaite, L., Tagle, D.A., Smith, S., Uziel, T., Sfez, S., Ashkenazi, M., Pecker, I., Frydman, M., Harnik, R., Patanjali, S.R., Simmons, A., Clines, G.A., Sartiel, A., Gatti, R.A., Chessa, L., Sanal, O., Lavin, M.F., Jaspers, N.G., Taylor, A.M., Arlett, C.F., Miki, T., Weissman, S.M., Lovett, M., Collins, F.S., Shiloh, Y., 1995. A single ataxia telangiectasia gene with a product similar to PI-3 kinase. Science 268, 1749–1753.
Shiloh, Y., Ziv, Y., 2013. The ATM protein kinase: regulating the cellular response to genotoxic stress, and more. Nat. Rev. Mol. Cell Biol. 14, 197–210.
Singh, V.V., Dutta, D., Ansari, M.A., Dutta, S., Chandran, B., 2013. Kaposi's sarcoma-associated herpesvirus induces ATM and H2AX DNA damage response early during de novo infection of primary endothelial cells which play roles in latency establishment. J. Virol..
Tarakanova, V.L., Leung-Pineda, V., Hwang, S., Yang, C.-W., Matatall, K., Basson, M., Sun, R., Piwnica-Worms, H., Sleckman, B.P., Virgin, H.W., 2007. Gammaherpesvirus kinase actively initiates a DNA damage response by inducing phosphorylation of H2AX to foster viral replication. Cell Host Microbe 1, 275–286.
Tarakanova, V.L., Molleston, J.M., Goodwin, M., Virgin IV, H.W., 2010. MHV68 complement regulatory protein facilitates MHV68 replication in primary macrophages in a complement independent manner. Virology 405, 50–61.
Tarakanova, V.L., Stanitsa, E., Leonardo, S.M., Bigley, T.M., Gauld, S.B., 2010. Conserved gammaherpesvirus kinase and histone variant H2AX facilitate gammaherpesvirus latency *in vivo*. Virology 405, 50–61.
Tarakanova, V.L., Suarez, F.S., Tibbetts, S.A., Jacoby, M., Weck, K.E., Hess, J.H., Speck, S.H., Virgin, H.W., 2005. Murine gammaherpesvirus 68 infection induces lymphoproliferative disease and lymphoma in BALB b2 microglobulin deficient mice. J. Virol. 79, 14668–14679.
Tibbetts, S.A., Van Dyk, L., Speck, S.H., Virgin, H.W., 2002. Immune control of the number and reactivation phenotype of cells latently infected with a gammaherpesvirus. J. Virol. 76, 7125–7132.
Virgin, H.W., Latreille, P., Wamsley, P., Hallsworth, K., Weck, K.E., Dal Canto, A.J., Speck, S.H., 1997. Complete sequence and genomic analysis of murine gammaherpesvirus 68. J. Virol. 71, 5894–5904.
Weck, K.E., Kim, S.S., Virgin, H.W., Speck, S.H., 1999a. B cells regulate murine gammaherpesvirus 68 latency. J. Virol. 73, 4651–4661.
Weck, K.E., Kim, S.S., Virgin, H.W., Speck, S.H., 1999b. Macrophages are the major reservoir of latent murine gammaherpesvirus 68 in peritoneal cells. J. Virol. 73, 3273–3283.
Ye, F., Zhou, F., Bedolla, R.G., Jones, T., Lei, X., Kang, T., Guadalupe, M., Gao, S.J., 2011. Reactive oxygen species hydrogen peroxide mediates Kaposi's sarcoma-associated herpesvirus reactivation from latency. PLoS. Pathog. 7, e1002054.
Zha, S., Sekiguchi, J., Brush, J.W., Bassing, C.H., Alt, F.W., 2008. Complementary functions of ATM and H2AX in development and suppression of genomic instability. Proc. Natl. Acad. Sci. U. S. A. 105, 9302–9306.
Zielonka, J., Hardy, M., Kalyanaraman, B., 2009. HPLC study of oxidation products of hydroethidine in chemical and biological systems: ramifications in superoxide measurements. Free. Radic. Biol. Med. 46, 329–338.